A poly(lactic acid)-based ink for biodegradable printed electronics with conductivity enhanced through solvent aging

*MADHUR ATREYA[†], KARAN DIKSHIT[§], GABRIELLE MARINICK[†], JENNA NIELSON[‡], CARSON BRUNS[†], GREGORY L WHITING[†§]**

†Paul M. Rady Department of Mechanical Engineering, University of Colorado Boulder

§Materials Science and Engineering Program, University of Colorado Boulder

‡Department of Chemical and Biological Engineering, University of Colorado Boulder.

***Corresponding author: gregory.whiting@colorado.edu.**

Keywords: Transient electronics, biodegradable sensors, conductive composites, printed electronics, physical aging

Abstract

Biodegradable electronics is a rapidly growing field, and the development of controllably biodegradable, high-conductivity materials suitable for additive manufacturing under ambient conditions remains a challenge. In this report, printable conductive pastes that employ poly(lactic acid) (PLA) as a binder and tungsten as a conductor are demonstrated. These composite conductors can provide enhanced stability in applications where moisture may be present, such as environmental monitoring or agriculture. Post-processing the printed traces using a solvent-aging technique increases their conductivity by up to two orders of magnitude, with final conductivities approaching 5000 S/m. Such techniques could prove useful when thermal processes including heating or laser sintering are limited by the temperature constraints of typical biodegradable substrates. Both accelerated oxidative and hydrolytic degradation of the printed composite conductors are examined, and a fully-biodegradable capacitive soil moisture sensor is fabricated and tested.

1.0 Introduction

Widely distributed electronic systems for environmental monitoring can enable the collection of large data sets useful for resource optimization in areas such as agriculture. However, the use of such sensor systems is limited by a number of factors including unit and maintenance cost, as well as the potential for creating significant amounts of persistent electronic waste in the environment.[1]

Research into transient electronic materials and devices has led to a number of available options for biodegradable conductive materials. However, development of biodegradable

high-conductivity materials suitable for additive manufacturing under ambient conditions remains a challenge, and typical biodegradable devices use conductive traces (e.g. magnesium, iron, zinc) deposited onto a biodegradable substrate (e.g. sodium carboxymethyl cellulose, silk, etc.) using methods such as chemical or physical vapor deposition (CVD or PVD).[2–5] Furthermore, these conductive traces are generally designed such that degradation occurs through aqueous dissolution, limiting long-term utility in environments with considerable moisture present (such as in soil).

In addition to these vapor deposited examples, pastes comprising conductive particles in degradable binders have also been demonstrated. For example, Huang et al. developed a screen printing ink consisting of tungsten particles in a poly(ethylene oxide) (PEO) in methanol binder**,** with in-plane conductivities reaching 5200 S/m.[2] When exposed to water, the PEO immediately dissolves, releasing tungsten particles, which slowly dissolve in water. While the primary application of this paste was to mount components, the authors demonstrated dissolution of a screen-printed antenna made from this same material within eight minutes. Similarly, in the context of transient batteries, Yin et al. use a molybdenum paste bound with sodium carboxymethylcellulose for interconnects between cells.[6] For biomedical applications, Lee et al. address the problem of fast dissolution of transient conductors by presenting a molybdenum-based screen printing ink in a UV-cured poly butanedithiol 1,3,5-triallyl-1,3,5-triazine-2,4,6(1H,3H,5H)-trione pentenoic anhydride binder.[7] These traces**,** with initial conductivities approaching 1400 S/m**,** lasted a maximum of nine days in deionized (DI) water at 37° C before they dissolved to an open circuit.

Traces printed from pastes often suffer from limited conductivity, therefore efforts have been made to post-process them in order to combat this. For example, Lee et al. proposed an ink comprising zinc in a poly(vinylpyrrolidone) (PVP) in isopropyl alcohol (IPA) binder.[8] Printed lines are then treated with an acetic acid/water solution in order to electrochemically sinter the zinc particles together at room temperature, increasing the conductivity by eight orders of magnitude to a final conductivity of 10^5 S/m. Traces degraded less than 10^4 S/m per day in ambient air and lasted for hours in water with the aid of a poly(lactic-co-glycolic acid) (PLGA) coating. Other processes include laser sintering[9] of zinc microparticle inks or the combination of hot rolling and photonic sintering[10] of zinc nanoparticle inks to increase their respective conductivities. Laser sintering improves conductivity by nine orders of magnitude with traces approaching a final conductivity of 9.7×10^5 S/m. Devices comprising these traces and a cellulose acetate encapsulant function for approximately one hour. Photonic sintering alone improves conductivity by one order of magnitude with one pulse, while the addition of hot rolling leads to a total increase of two orders of magnitude with traces exceeding 6×10^4 S/m. These traces fully dissolve in 25 minutes.

In printed electronics and conductive polymer composites literature, densification of the binder due to cross-linking or drying is often cited as a reason for conductivity increase.[2,7] However, even after cooling or drying a polymer/conductor composites, the binder may not be at thermodynamic equilibrium.[11–16] Annealing at temperature ranges above the glass transition temperature (T_g) of the binder material can lead to increases in conductivity. For example, polymer composites consisting of carbon black tend to increase in conductivity when samples are physically constrained between plates and held at temperatures including those

above the melting temperature.[12,13,15] In addition, conductivity of high-aspect ratio anisotropic particles such as carbon nanotubes can be improved through pre- and post-processing alignment techniques.[17]

Physical aging is a process occurring below or near T_g wherein a polymer moves towards thermodynamic equilibrium, reducing its enthalpy, entropy, and, most importantly for conductive composites, its specific volume.[18] Physical aging has been explored for composites of PEO, lithium perchlorate, and aluminum oxide, in order to improve ionic conductivity for fuel cell electrolyte applications.[11] Structural densification that results from the heating treatment is attributed as the cause of the improved conductivity.

Here, we demonstrate printable biodegradable conductive pastes that employ poly(lactic acid) (PLA) as a binder, in order to provide improved stability in environments with water present. We also employ a post-processing technique to increase conductivity by utilizing the tendency for PLA to undergo physical aging in the presence of solvents such as water.[19,20] This technique can increase conductivity of the printed composite by two orders of magnitude, and is expected to be particularly useful for applications wherein the sintering temperature of metal microparticles is too high for use on biodegradable substrates. PLGA has been previously used as a binder[7] but has seen limited development and investigation. While poly(lactic acid) (PLA) (or the related PLGA) will eventually degrade due to hydrolysis in aqueous environments,[21] its degradation can be accelerated in the presence of an enzyme such as bromelain or proteinase K.[22–27] Prescribed degradation rates can also be tuned by adjusting the molecular weight and the lactide-to-glycolide ratio,[28] with lower crystallinity and lower molecular weight yielding faster biodegradation rates.[19,23,29] A higher lactide content, on the other hand, slows hydrolytic

degradation by making the polymer more hydrophobic.[28] These characteristics render PLA a useful and tunable binder for printed, biodegradable electronics.

In addition, we employ a robotic material extrusion method wherein a viscous PLA solution with conductive metal particles is deposited from a rotary screw driven syringe-needle assembly.[30–34] This can then be integrated with other additive manufacturing techniques such as fused deposition modeling (FDM), to eventually aid in the production of complex geometries. However, such an ink can be readily modified for use in screen and stencil printers, enabling the deposition of a wide range of materials, thus allowing for low-cost, scalable manufacturing.

2.0 Experimental Section

2.1 Ink Formulation

NatureWorks Ingeo Biopolymer 10361D PLA pellets [which consist principally of poly(l-lactic) acid (PLLA)], were stored in vacuum at 45 °C for at least 24 hours prior to use. The pellets were then dissolved in tetrahydrofuran (THF) at a concentration of 167 mg/mL with stirring at 40 °C and stored in a sealed bottle at room temperature. Tungsten powder (Sigma-Aldrich, 12 μm, and Inframat Advanced Materials, 4-6 μm) was added at a concentration of 3.33 g/ml, and mixed using a vortexer to formulate the final print inks. Inks and printed traces consisting of 12 μm particles will henceforth be referred to as PLA-W12, and those consisting of 4-6 μm particles will be referred to as PLA-W6. The viscosities of the resultant inks (measured using a shear rheometer [Anton Paar MCR 301]) are 31,100 mPa.s for PLA-W6 and 7,250 mPa.s for PLA-W12 at a shear rate of 10 s^{-1} (see Figure S1 for flow curves).

2.2 Printing and Processing of Conductive Traces

Robotic material extrusion was selected as the method of printing to enable rapid digital prototyping of viscous inks with high-mass loading of conductive tungsten particles. Samples were printed using a Hyrel Engine SR multi-process 3D printer with a syringe and luer-lock 18 gauge blunt needle. Traces were printed on glass microscope slides. After printing, samples were placed in a vacuum oven and allowed to dry for at least 24 hours in 45 °C dynamic vacuum. After initial drying, the samples consisting of both particle sizes were placed in individual covered containers of room-temperature reverse osmosis (RO) filtered water and then placed inside a 37 °C incubator for time intervals ranging from 3 to 36 hours in order to age the PLA binder and increase conductivity. This aging process was then repeated for PLA-W12 with shorter timescales using a one-to-one by volume ethanol and water solution.[19]

Soaked samples were placed back in the vacuum oven for at least 48 hours. Volume resistivity of the traces were then determined using a Keithley 2450 SourceMeter to measure resistance, a digital micrometer to measure thickness, and digital calipers to measure line width and length.

2.3 Thermal characterization of the printed traces

Thermal characterization was carried out on PLA-W samples using differential scanning calorimetry (DSC) (Q2000, TA Instruments). Printed traces were soaked at different times varying from 3 hours to 48 hours. In addition, PLA films, which were spin cast onto microscope slides from a similar solution of PLA in THF, and soaked in water, were thermally characterized as a control. All printed samples (weights varying between 4-10 mg) were equilibrated at 0 °C and heated to 200 °C, higher than the melting point of the as-obtained PLA, at a rate of 10 °C/min.

2.4 Microscopy and Mass Spectroscopy

In order to further investigate the cause of the increased conductivity in PLA-W samples, scanning electron microscope (SEM) (SU3500, Hitachi) images were taken of PLA-W6 and PLA-W12 traces pristine traces, and traces subject to 24 hours of soaking in RO water. Cross sections were obtained by submerging traces in liquid nitrogen before sectioning. Samples were sputtered with platinum prior to observation.

Electrospray ionization (ESI) mass spectroscopy (positive and negative) (Synapt G2 QToF High-Resolution Mass Spectrometer, Waters) was also conducted on the RO water used to soak a 12 μm printed trace for 24 hours. The water was not purified before submitting it for analysis.

2.5 Rapid Degradation Test Method

Samples were wired to a Keithley 2450 electrometer and placed in a beaker inside an incubator and stirred at 37 °C. The beakers contained either 30 ml of 30% hydrogen peroxide (H_2O_2) for oxidation tests, or 30 ml Tris-HCl buffer (0.05 M, pH 8.6) with approximately 15 mg of the enzyme proteinase K for enzymatic degradation tests. The enzyme concentration of 0.5 mg/ml is more than doubled as compared to the more common concentration of 0.2 mg/ml in order to further accelerate degradation.[23–27] Both liquids were initially at room temperature before beginning tests. These experiments were repeated in RO water at room temperature, pre-warmed RO water at 37 °C, and air at 37 °C. Resistance for each sample was normalized by dividing by the initial resistance. The electrometer samples approximately every .069 seconds, but for ease of plotting and processing data, data sets were condensed by taking every 2500th sample. Warm air

and room temperature water samples were measured once or twice a day for at least a week with either a Keithley 2450 electrometer or Fluke 179 digital multimeter.

We included a mass loss study in oxidative conditions since oxidative attack of printed conductive traces can be better tracked through time than hydrolysis of the binder, which simply leads to tungsten particles being released. For these mass loss studies, a vial of H_2O_2 with approximately 100 mg of sample was placed on a hotplate stirrer set at 42 °C (the H_2O_2 and test samples were at room temperature when placed on the hotplate to reduce H_2O_2 degradation before the beginning of the test).

2.6 Soil Moisture Testing

In order to demonstrate the viability of integrating our conductive ink into a multi-process additive manufacturing procedure, we fabricated a capacitive soil moisture sensor using the ink described above. PLA-W12 conductive traces, approximately 2.5 mm in width, were printed onto FDM-printed PLA substrates (TIANSE, Orange PLA 3D Printer Filament, 1.75mm). After completing the aging process, the samples were then encapsulated in biodegradable packing tape (TRU CELLO) and dip coated in PLA in chloroform (0.17 g/ml) as a biodegradable encapsulation.

Consumer potting soil was dried for 72 hours at 120 °C and stored in a covered beaker at room temperature. The sensor was placed in a cup of this soil and connected to a Keysight E4980A LCR meter. Water was added to the surface of the soil using a micropipette. Capacitance measurements were taken at 2 V and 1 kHz using the two wire method and measurements were recorded approximately 5 minutes after the addition of water. This voltage

and frequency were selected by iterating and testing the sensor in water and air and selecting the parameters that led to the greatest sensitivity.

3.0 Results and Discussion

3.1 Electrical characterization of printed trace

In polymer-metal composites such as the ones presented here, conductivity is achieved by the development of a number of percolation pathways between the conductive particles (see Figure 1A).[7,12,13,15] During service life, the binder protects the geometric stability of the trace and prevents oxidation of the conductive particles. In the presence of a solvent such as water, the binder may swell, reducing the number of percolation pathways (Figure 1B). Once the binder is degraded, conductive particles are released and can degrade at a faster rate than bulk metal, due to their higher surface area providing increased contact with the solvent. This degradation route is illustrated in Figure 1C and 1D.

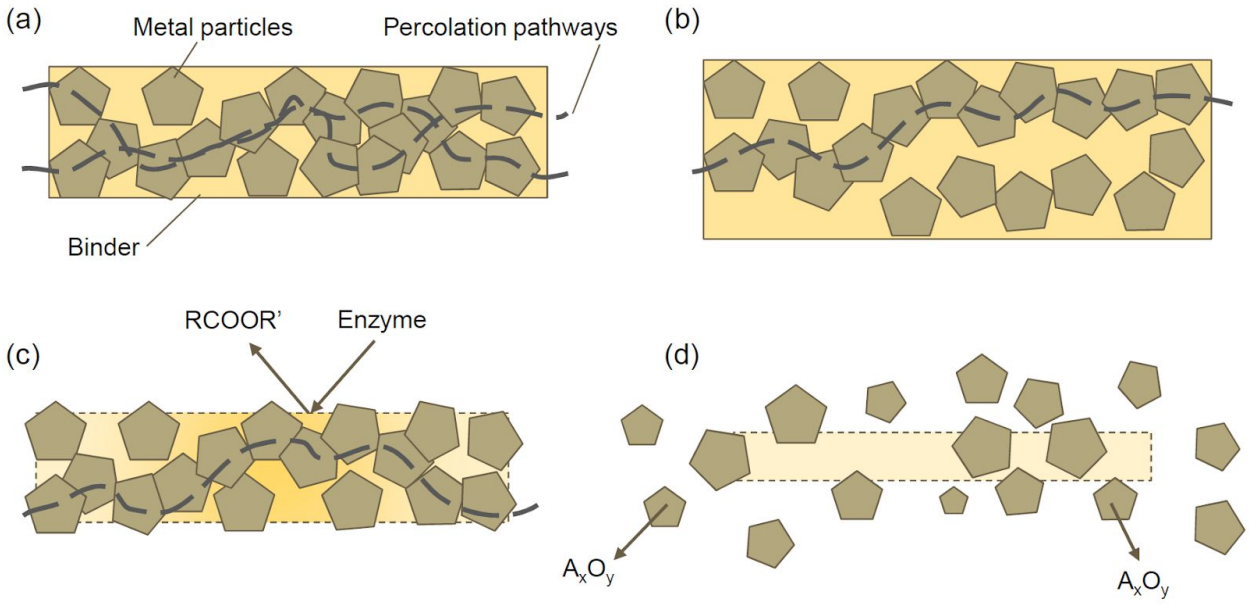

Figure 1: (a) Structure of a typical printed conductive line consisting of metal particles and a degradable binder; (b) Swelling (exaggerated for clarity) can reduce the number of percolation pathways; (c) An enzyme accelerates hydrolysis of the binder; (d) Released particles can oxidize and dissolve.

Tungsten affords several advantages in its role as the active material for ambiently printable conductive biodegradable inks, and has previously been used in water soluble screen printing inks.[2] Other materials, such as zinc and iron powders can also be used, but typically show lower conductivity in traces due to the formation of native oxide layers.[2,7] To make a printable, biodegradable, conductive trace with enhanced water and air stability, tungsten powder with a 6 μm and 12 μm particle size was blended with PLA. A 5 wt.% of PLA to tungsten ratio was selected to bind the particles in the trace, provide appropriate viscosity to suspend the tungsten particles, and give appropriate rheological properties for printing. PLA is relatively insoluble in water compared with polymers such as PEO, more readily enabling these traces to operate in environments where water is present without immediately degrading. In the final printed trace, the water solubility of the tungsten particles is expected to be initially reduced due to the presence of the binder, reducing tungsten surface area accessible to the solvent. Printing of the inks was carried out through a robotic material extrusion process, where the viscous ink is forced through a needle and translated across the substrate surface to create the printed structure. While a digital process was used here, these paste-like inks are also suitable for master-based print processes such as screen printing.

As-printed PLA-W traces displayed a volume resistivity of 3.85 to 8.78 Ω·cm for traces containing 12 μm tungsten (PLA-W12) and 0.22 to 0.60 Ω·cm for traces containing 6 μm particles (PLA-W6). The process of aging PLA-W traces in water significantly decreased their volume resistivity. Tables S1 and S2 tabulate average resistivity values before and after soaking for times ranging from 3 to 48 hours, and Figure 2A illustrates the percent change in resistivity

as a function of aging time in water. After submerging printed and dried samples in water, a decrease in resistivity of about 2 orders of magnitude was observed for PLA-W12 traces and 1 order of magnitude for PLA-W6 traces, with a final volume resistivity as low as 0.02 Ω·cm (for a PLA-W6 sample). The observation that PLA-W12 samples decrease in resistivity more than PLA-W6 samples, with respect to their as-printed resistivity, could be explained by the fact that initial inter-particle distance in a composite increases with particle size.[35,36] Therefore, reductions in specific volume of the binder from physical aging may lead to more drastic drops in resistivity before reaching a minimum, particularly since electron tunneling through the binder material is considered in percolation pathways.[35] However, for the same mass fraction and processing conditions, PLA-W12 traces would be expected to have a higher resistance than PLA-W6 traces due to the positive correlation between particle size and resistivity.[28,35,36] The decrease in resistivity occurs principally within the first six hours of aging in pure water, and stabilizes over longer times (beyond 12 hours). It was observed with PLA-W12 samples that this process can be accelerated by soaking the traces in a 50/50 mixture of water and ethanol rather than pure water (10-30 minutes).[19] However, in this solution, the process was noted to be somewhat unreliable as damage to the trace and delamination from the substrate also occurred. The origin of these observed resistance changes was further studied through thermal characterization of the composites.

3.2 Thermal Characterization

The presence of endothermic peaks at the glass transition temperature (T_g) of PLA are observed using differential scanning calorimetry (DSC). PLA is a slow-crystallizing polymer; having a considerable amorphous, glassy component.[37] Although the samples were soaked in

solvents below the T_g of the polymer, where the kinetics of chain mobility are significantly hindered, molecular mobility still exists.[38] The pervasive molecular motions cause structural rearrangement also referred to as physical aging. Physical aging is driven by the slow evolution of thermodynamic properties (such as specific volume, entropy, enthalpy) towards the equilibrium solid line.[18] Previous aging experiments with composites of PLA are conducted on orders of hundreds of hours.[14] The plasticizing effect of various solvents (including water) has been reported for PLA, which would ensure that the polymer undergoes structural rearrangement on much shorter time scales.[19,20,39,40] Lowering of glass transition is observed for unsoaked PLA film as well as the PLA soaked in water for 24 hours, whereas the printed trace shows no depression in T_g but rather an endothermic peak associated with aging in polymers. The printed trace is composed mostly of tungsten particles which may potentially confine the small amount of PLA chains present, leading to aging in the print and not the plasticization shown for the pure PLA film (Figure 2B).

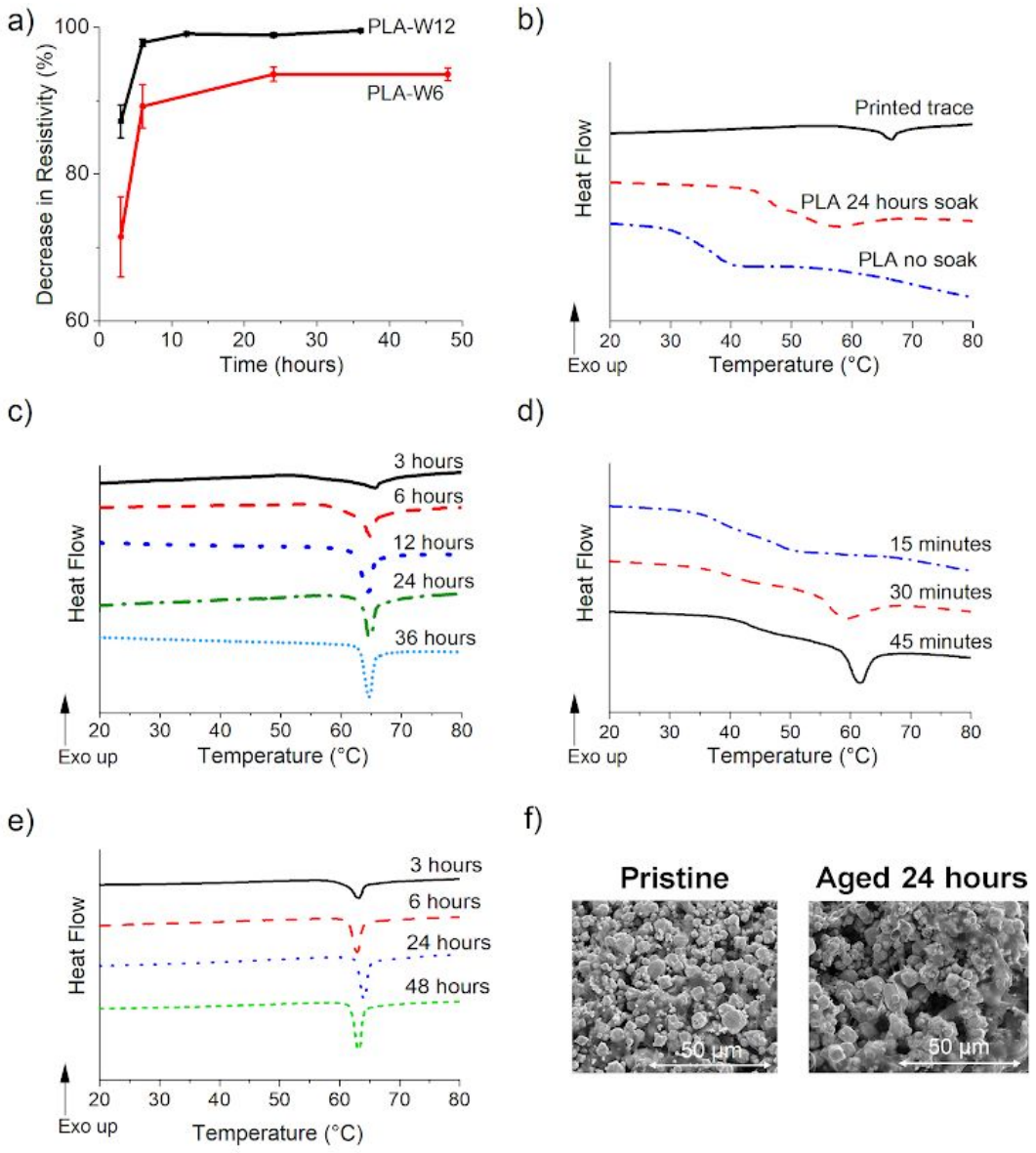

Figure 2: a) Decrease in volume resistivity of printed traces as a function of time aged in RO water. b) DSC heating run of pure PLA film (unsoaked and soaked for 24 hours in water) and printed trace (unsoaked); c) DSC heating runs indicating the increase in aging of PLA-W12 traces in water as soak time increases; d) DSC heating runs indicating aging of PLA-W12 printed traces in a mixture of ethanol and water soaked for varying amounts of time; e) DSC heating runs indicating the increase in aging of PLA-W6 traces in water as soak time increases. f) Microstructure of pristine and aged PLA-W6 traces.

Longer soaking times of PLA in water leads to more aging,[20] which has been corroborated by our results (Figure 2C and E). The increase in enthalpy values, indicated by the endothermic peaks, with increasing soak time suggests that the polymer continues rearranging in the printed trace. Prior to aging, the PLA occupies a larger specific volume in the substrate, leading to higher resistance. Aging of PLA reduces the specific volume,[41] suggesting closer packing of the tungsten particles. The printed substrate was also exposed to another solvent system (ethanol + water), albeit for a shorter time, to confirm solvent assisted aging. Endothermic peaks, without a depression in T_g, in this solvent system also indicate aging in the printed traces, which confirms that solvent assisted physical aging does occur in the printed traces. Exposing PLA to ethanol causes softening of the polymer leading to chain mobility and realignment[19] which manifests as physical aging. (Figure 2D). Changing particle size also affects how the confined polymer ages as observed in the heat of fusion and rate of aging. Compared to 12 μm particles (Figure 2C), traces printed with 6 μm tungsten particles (Figure 2E) show rapid aging with higher enthalpy values as has been indicated in Table S3.

3.4 SEM and ESI Mass spectrometry results

Scanning electron microscope (SEM) images were taken for both pristine and aged traces (see Figure 2F for PLA-W6 microstructure, see Figure S2 for all images). Inter-particle structural changes, such as sintering, were not apparent in these images. The reduction in specific volume associated with aging has been well reported for PLA,[42] as well the effect of enhanced physical aging due to hydration.[20] SEM images of both PLA-W6 and PLA-W12 traces show a lack of long range (crystalline) order after carrying out the solvent aging process. The absence of visible

crystalline domain buildup, as seen by SEM, along with lack of a melting peak in DSC confirm aging in PLA, rather than annealing.

Volume shrinkage due to physical aging of polymers has been reported earlier,[43] including for PLA[44] and its composites.[14,16] Measurements of the outer dimensions of the conductive traces before and after soaking showed no obvious change. However, cross-sectional SEM analysis revealed an apparent increase in the presence of voids in the microstructure of the trace after soaking. This could suggest that the reduction of specific volume is manifested as internal contractions of the PLA matrix leading to the clustering of W particles, and a corresponding increase in conductivity.

Waters MassLynx 4.1 software was used to analyze the spectra resulting from ESI mass spectrometry for the presence of possible chemical compounds in the water used to age PLA-W samples. By comparing the resulting spectra to spectra for possible compounds, the presence of lactic acid in the water was confirmed with the positive spectra (see Figure S3 for the spectra). ESI has been used in previous literature to confirm the presence of lactic acid oligomers in solutions that were used to soak PLA packaging.[45] Lactic acid in the water confirms that hydrolysis of the PLA is occurring simultaneously to the solvent assisted physical aging. As an extension of this observation, hydrolysis is likely one of the causes of the eventual failure of the trace during degradation studies. In addition, this observation suggests another possible mechanism that could contribute to the increase in conductivity observed when the sample is soaked in water for extended times, since an acid solution may etch the native oxide layer from the tungsten particles, potentially leading to increased particle-particle contact.

3.5 Degradation Studies

Transient conductive traces consisting of metal particles and a biodegradable binder will eventually degrade as a result of two main failure modes: hydrolysis and/or dissolution of the binder, and oxidation and dissolution of the conductive particle in the presence of water. Current soil biodegradation tests of polymers typically rely on controlled composting methods or actual burial in soil with experimental timescales ranging from several weeks to months.[27,46–48] Factors such as mass, mechanical strength, crystallinity, CO_2 evolution, and/or molecular weight are measured afterwards. These time scales prohibit rapid iteration of sensor design and materials.

Under expected environmental conditions, the binder will be degraded and then solubilized with the help of extracellular depolymerase produced by microbial activity. The tungsten particles are then released, exposing their full surface area, allowing them to dissolve more rapidly in water. Therefore, in order to develop an accelerated degradation testing methodology, we chose to separate the two processes into extreme oxidative conditions: accelerated by the presence of hydrogen peroxide and extreme hydrolytic conditions or accelerated by the presence of an enzyme.

In deionized water at room temperature, sputter deposited tungsten has been shown to dissolve at a rate of 1.7×10^{-3} μm/h, while CVD tungsten has been shown to dissolve at 3×10^{-4} μm/h, which suggests complete dissolution times (in RO water) for 12 μm particles on the order of 100 days.[3] Furthermore, it is expected that the presence of binders such as PLA will decrease the tungsten dissolution time by reducing available solvent/metal surface area. While these degradation times are suitable for many soil monitoring applications, for iterative experimental studies, accelerated characterization is desirable. In order to rapidly study the binder impact on

degradation of the tungsten trace, tests were carried out under oxidative conditions by submerging tungsten powders and the printed and solvent aged traces (without their respective substrates) in a beaker of room temperature 30% hydrogen peroxide and stirring it on a hotplate at 42° C (n=3 per sample per time).

Under these conditions, 100 mg of agitated tungsten powder is completely dissolved after about 120 minutes (see Figure 3A), with PLA pellets showing negligible change in mass over a span of 2 hours. For PLA-W traces initially containing roughly 100 mg of 12 μm W, 22% remained after 2 hours, and for traces initially containing roughly 100 mg of 6 μm W, 10% remained. These results are illustrated in Figure 3A, and demonstrate that, as expected, the presence of binder in the composite trace slows dissolution. Measurement errors for powder samples could have resulted from loss of remaining powder while decanting hydrogen peroxide and water used for rinsing. Errors for composite traces likely resulted from variations in trace geometry. While hydrogen peroxide is known to eventually degrade PLA,[49] negligible degradation is seen at this time span and temperature.

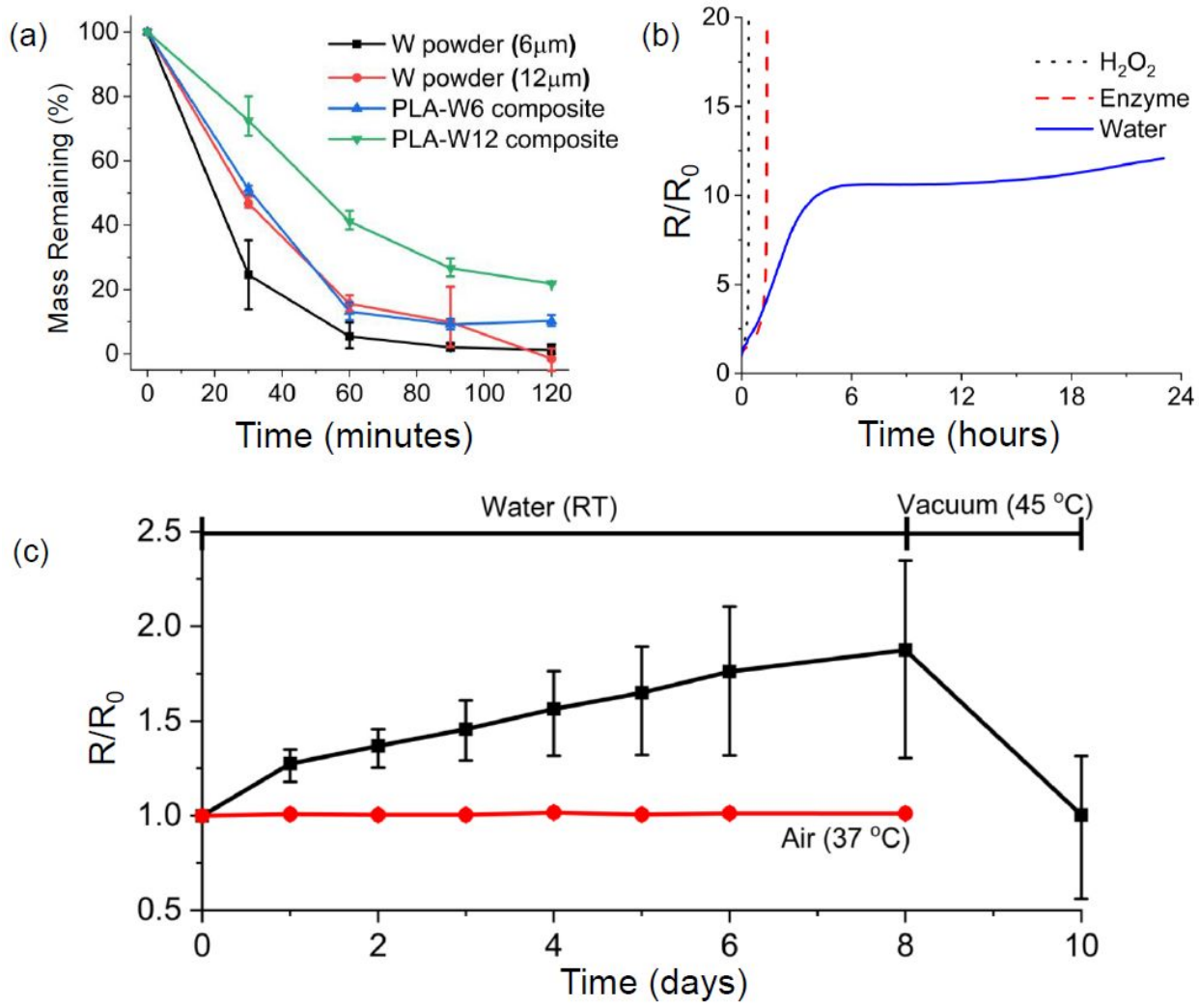

Figure 3: a) Mass loss studies of 100 mg tungsten powder and 100 mg of printed and aged PLA-W traces. b) Resistance behavior of PLA-W6 prints in water, hydrogen peroxide, and enzyme. c) Resistance behavior of PLA-W6 prints observed in 37 °C air and room temperature water over a week.

Degradation of printed traces was also evaluated by carrying out studies tracking their resistance under accelerated conditions. Samples 150 mm in length and approximately 2 mm wide were printed on glass, vacuum dried, aged for 24 hours, re-dried for at least 48 hours, and placed in beakers containing appropriate fluids at the desired temperature (37 °C) and the resistance was monitored over time.

Figure 3B shows the typical behavior of 3 different PLA-W6 traces in 37 °C pre-warmed RO water, hydrogen peroxide, and proteinase K enzyme and buffer solution. As expected, the trace placed in H_2O_2 failed relatively quickly due to oxidation and dissolution of the tungsten, with normalized resistance approaching open circuit within approximately 15 minutes. The normalized resistance of the trace placed in enzyme/buffer solution approached an open circuit at about 80 minutes, with the submerged portion of the trace visibly disintegrated. Note the initial tenfold increase in resistance of the trace in pre-warmed RO water. This sample was removed from water after approximately 24 hours and dried in the vacuum oven for another 48 hours. The process of re-drying this sample brought it back to below its starting resistance, implying that the main mechanism leading to increased resistance at these time scales is likely swelling and aging, rather than hydrolysis.

PLA-W6 traces (n=3 per point, per experiment) were also placed in room temperature water and in air at 37 °C (see Figure 3C) and monitored for at least a week. The traces placed in room temperature water experienced an initial 27% jump in resistance within the first day, and slowly increased to 87% above initial resistance over a total of eight days. Re-drying these samples significantly reduced the resistance, likely due to the fact that aging occurs at a much slower rate at lower temperatures.[38] PLA-W6 traces only increased in resistance by an average of 1% after being placed in 37° C ambient air for seven days, suggesting that increases in resistance in warm water were not caused simply by increase in temperature.

4.0 Soil Moisture Sensor

Soil capacitance is a common indicator of soil moisture and has been utilized for this purpose for a few decades.[50–52] An advantage of using capacitance rather than resistance is that

electrodes do not have to be exposed to the soil. Thus, corrosion and electrolysis is not a concern. A single 260 mm trace of PLA-W12, approximately 2.5 mm wide, was printed in one operation on an FDM PLA substrate, and the end was manually cut to yield two conductors. Sensors were aged in RO water for 24 hours, vacuum dried, and then wrapped in biodegradable cellulose tape and dip coated in solutions of PLA. Figures 4A and 4B respectively show a cross-section drawing and photo of a printed, fully biodegradable, soil moisture sensor packaged in cellulose and PLA. Figure 4C demonstrates the result of the tests conducted with such sensors at 2 V and 1kHz. The test was conducted twice with Sensor 1 and once with Sensor 2, which was damaged after the first run.

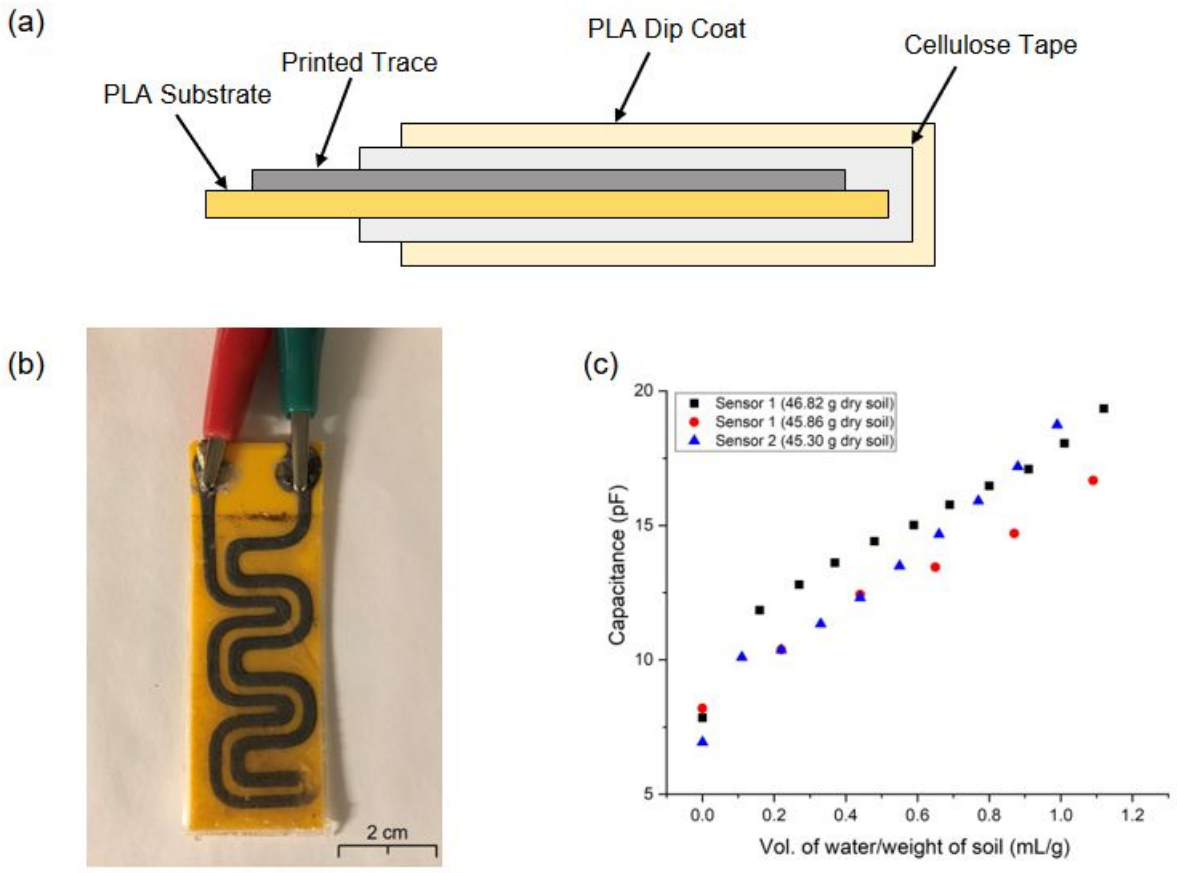

Figure 4: a) Soil moisture sensor cross-section; b) Example soil moisture sensor; and c) Results of example soil moisture sensor testing.

5.0 Conclusion and Future Work

We have developed PLA-based conductive biodegradable inks that can be readily printed with the robotic material extrusion method. Soaking these conductive traces in the presence of water and/or ethanol for a limited time aids in increasing conductivity up to two orders of magnitude. Loss of conductivity when traces were exposed to water tended to be partially reversible simply by drying. This could allow conductive traces to tolerate a limited number of wet-dry cycles such as those seen in soil, without significant degradation. We also demonstrated that degradation can be accelerated in the presence of an oxidizing agent such as hydrogen peroxide or esterase enzymes such as proteinase K. Future work in this area could evaluate other options for polymer binders [such as poly(hydroxyalkanoates)], and conductors including magnesium, iron or carbon. In addition, a solvent aging or annealing technique can be applied to other polymers that exhibit behavior similar to PLA. Optimization of encapsulating layers, and fabrication of fully functional printed, biodegradable, soil moisture sensors and systems will also be explored.

Associated Content

Flow curves for PLA-W6 and PLA-W12, volume resistivity information for both inks before and after aging for various times, additional SEM micrographs, and ESI+ mass spectrometry results.

Author Information

Corresponding Author: *E-mail: gregory.whiting@colorado.edu

The authors declare no competing financial interests.

Acknowledgements

This work was funded by the Advanced Research Projects Agency - Energy (ARPA-E) Award: DE-AR0001013. Additionally, portions of this work were funded by the Mechanical Engineering Department and the College of Engineering and Applied Science (CEAS) at the University of Colorado, Boulder through startup funds. We would like to thank the Discovery Learning Apprenticeship (DLA) Program and the Summer Program for Undergraduate Research (SPUR) in CEAS at the University of Colorado Boulder for providing funding for Undergraduate researchers involved in the project. We would also like to thank the Colorado Shared Instrumentation in Nanofabrication and Characterization facility (COSINC) at the University of Colorado Boulder for use of their SEM and Prof. Wil Srubar and the students of the Living Materials Laboratory at the University of Colorado Boulder for allowing us time on their differential scanning calorimeter.

(1) Mukhopadhyay, S. C.; Suryadevara, N. K. Internet of Things: Challenges and Opportunities. In *Internet of Things*; Mukhopadhyay, S. C., Ed.; Springer International Publishing: Cham, 2014; Vol. 9, pp 1–17. https://doi.org/10.1007/978-3-319-04223-7_1.
(2) Huang, X.; Liu, Y.; Hwang, S.-W.; Kang, S.-K.; Patnaik, D.; Cortes, J. F.; Rogers, J. A. Biodegradable Materials for Multilayer Transient Printed Circuit Boards. *Adv. Mater.* **2014**, *26* (43), 7371–7377. https://doi.org/10.1002/adma.201403164.
(3) Yin, L.; Cheng, H.; Mao, S.; Haasch, R.; Liu, Y.; Xie, X.; Hwang, S.-W.; Jain, H.; Kang, S.-K.; Su, Y.; Li, R.; Huang, Y.; Rogers, J. A. Dissolvable Metals for Transient Electronics. *Adv. Funct. Mater.* **2014**, *24* (5), 645–658. https://doi.org/10.1002/adfm.201301847.
(4) Kang, S.-K.; Park, G.; Kim, K.; Hwang, S.-W.; Cheng, H.; Shin, J.; Chung, S.; Kim, M.; Yin, L.; Lee, J. C.; Lee, K.-M.; Rogers, J. A. Dissolution Chemistry and Biocompatibility of Silicon- and Germanium-Based Semiconductors for Transient Electronics. *ACS Appl. Mater. Interfaces* **2015**, *7* (17), 9297–9305. https://doi.org/10.1021/acsami.5b02526.
(5) Tao, H.; Brenckle, M. A.; Yang, M.; Zhang, J.; Liu, M.; Siebert, S. M.; Averitt, R. D.; Mannoor, M. S.; McAlpine, M. C.; Rogers, J. A.; Kaplan, D. L.; Omenetto, F. G. Silk-Based Conformal, Adhesive, Edible Food Sensors. *Adv. Mater.* **2012**, *24* (8), 1067–1072. https://doi.org/10.1002/adma.201103814.
(6) Yin, L.; Huang, X.; Xu, H.; Zhang, Y.; Lam, J.; Cheng, J.; Rogers, J. A. Materials, Designs, and Operational Characteristics for Fully Biodegradable Primary Batteries. *Adv. Mater.* **2014**, *26* (23), 3879–3884. https://doi.org/10.1002/adma.201306304.
(7) Lee, S.; Koo, J.; Kang, S.-K.; Park, G.; Lee, Y. J.; Chen, Y.-Y.; Lim, S. A.; Lee, K.-M.; Rogers, J. A. Metal Microparticle – Polymer Composites as Printable, Bio/Ecoresorbable Conductive Inks. *Mater. Today* **2018**, *21* (3), 207–215. https://doi.org/10.1016/j.mattod.2017.12.005.
(8) Lee, Y. K.; Kim, J.; Kim, Y.; Kwak, J. W.; Yoon, Y.; Rogers, J. A. Room Temperature Electrochemical Sintering of Zn Microparticles and Its Use in Printable Conducting Inks for Bioresorbable Electronics. *Adv. Mater.* **2017**, *29* (38), 1702665. https://doi.org/10.1002/adma.201702665.
(9) Feng, S.; Tian, Z.; Wang, J.; Cao, S.; Kong, D. Laser Sintering of Zn Microparticles and Its Application in Printable Biodegradable Electronics. *Adv. Electron. Mater.* **2019**, *5* (3), 1800693. https://doi.org/10.1002/aelm.201800693.
(10) Li, J.; Luo, S.; Liu, J.; Xu, H.; Huang, X. Processing Techniques for Bioresorbable Nanoparticles in Fabricating Flexible Conductive Interconnects. *Materials* **2018**, *11* (7), 1102. https://doi.org/10.3390/ma11071102.
(11) Kumar, B. Physical Aging Effects on Conductivity in Polymer Electrolytes. *Solid State Ion.* **2003**, *156* (1–2), 163–170. https://doi.org/10.1016/S0167-2738(02)00610-0.
(12) Wu, G.; Asai, S.; Zhang, C.; Miura, T.; Sumita, M. A Delay of Percolation Time in Carbon-Black-Filled Conductive Polymer Composites. *J. Appl. Phys.* **2000**, *88* (3), 1480–1487. https://doi.org/10.1063/1.373843.
(13) Deng, H.; Skipa, T.; Zhang, R.; Lellinger, D.; Bilotti, E.; Alig, I.; Peijs, T. Effect of Melting and Crystallization on the Conductive Network in Conductive Polymer Composites. *Polymer* **2009**, *50* (15), 3747–3754. https://doi.org/10.1016/j.polymer.2009.05.016.

(14) Lizundia, E.; Pérez-Álvarez, L.; Sáenz-Pérez, M.; Patrocinio, D.; Vilas, J. L.; León, L. M. Physical Aging and Mechanical Performance of Poly(ʟ -Lactide)/ZnO Nanocomposites. *J. Appl. Polym. Sci.* **2016**, *133* (45). https://doi.org/10.1002/app.43619.
(15) Zhang, C.; Wang, P.; Ma, C.; Wu, G.; Sumita, M. Temperature and Time Dependence of Conductive Network Formation: Dynamic Percolation and Percolation Time. *Polymer* **2006**, *47* (1), 466–473. https://doi.org/10.1016/j.polymer.2005.11.053.
(16) Lizundia, E.; Sarasua, J. R. Physical Aging in Poly(L-Lactide) and Its Multi-Wall Carbon Nanotube Nanocomposites. *Macromol. Symp.* **2012**, *321–322* (1), 118–123. https://doi.org/10.1002/masy.201251120.
(17) Goh, G. L.; Agarwala, S.; Yeong, W. Y. Directed and On-Demand Alignment of Carbon Nanotube: A Review toward 3D Printing of Electronics. *Adv. Mater. Interfaces* **2019**, *6* (4), 1801318. https://doi.org/10.1002/admi.201801318.
(18) Hodge, I. M. Physical Aging in Polymer Glasses. *Science* **1995**, *267* (5206), 1945–1947.
(19) Iñiguez-Franco, F.; Auras, R.; Burgess, G.; Holmes, D.; Fang, X.; Rubino, M.; Soto-Valdez, H. Concurrent Solvent Induced Crystallization and Hydrolytic Degradation of PLA by Water-Ethanol Solutions. *Polymer* **2016**, *99*, 315–323. https://doi.org/10.1016/j.polymer.2016.07.018.
(20) Vyavahare, O. V. Investigation of Hydration Induced Structural Rearrangements of Poly(Lactic Acid), University of Massachusetts Amherst, 2015.
(21) Qi, X.; Ren, Y.; Wang, X. New Advances in the Biodegradation of Poly(Lactic) Acid. *Int. Biodeterior. Biodegrad.* **2017**, *117*, 215–223. https://doi.org/10.1016/j.ibiod.2017.01.010.
(22) Williams, D. F. Enzymic Hydrolysis of Polylactic Acid. *Eng. Med.* **1981**, *10* (1), 5–7. https://doi.org/10.1243/EMED_JOUR_1981_010_004_02.
(23) Reeve, M. S.; McCarthy, S. P.; Downey, M. J.; Gross, R. A. Polylactide Stereochemistry: Effect on Enzymic Degradability. *Macromolecules* **1994**, *27* (3), 825–831. https://doi.org/10.1021/ma00081a030.
(24) Li, S.; Tenon, M.; Garreau, H.; Braud, C.; Vert, M. Enzymatic Degradation of Stereocopolymers Derived from l -, Dl - and Meso-Lactides. *Polym. Degrad. Stab.* **2000**, *67* (1), 85–90. https://doi.org/10.1016/S0141-3910(99)00091-9.
(25) Tuominen, J.; Kylmä, J.; Kapanen, A.; Venelampi, O.; Itävaara, M.; Seppälä, J. Biodegradation of Lactic Acid Based Polymers under Controlled Composting Conditions and Evaluation of the Ecotoxicological Impact. *Biomacromolecules* **2002**, *3* (3), 445–455. https://doi.org/10.1021/bm0101522.
(26) Luzi, F.; Fortunati, E.; Puglia, D.; Petrucci, R.; Kenny, J. M.; Torre, L. Study of Disintegrability in Compost and Enzymatic Degradation of PLA and PLA Nanocomposites Reinforced with Cellulose Nanocrystals Extracted from Posidonia Oceanica. *Polym. Degrad. Stab.* **2015**, *121*, 105–115. https://doi.org/10.1016/j.polymdegradstab.2015.08.016.
(27) Hu, X.; Su, T.; Li, P.; Wang, Z. Blending Modification of PBS/PLA and Its Enzymatic Degradation. *Polym. Bull.* **2018**, *75* (2), 533–546. https://doi.org/10.1007/s00289-017-2054-7.
(28) Hwang, S.-W.; Song, J.-K.; Huang, X.; Cheng, H.; Kang, S.-K.; Kim, B. H.; Kim, J.-H.; Yu, S.; Huang, Y.; Rogers, J. A. High-Performance Biodegradable/Transient Electronics on Biodegradable Polymers. *Adv. Mater.* **2014**, *26* (23), 3905–3911. https://doi.org/10.1002/adma.201306050.

(29) Pantani, R.; Sorrentino, A. Influence of Crystallinity on the Biodegradation Rate of Injection-Moulded Poly(Lactic Acid) Samples in Controlled Composting Conditions. *Polym. Degrad. Stab.* **2013**, *98* (5), 1089–1096. https://doi.org/10.1016/j.polymdegradstab.2013.01.005.
(30) Espera, A. H.; Dizon, J. R. C.; Chen, Q.; Advincula, R. C. 3D-Printing and Advanced Manufacturing for Electronics. *Prog. Addit. Manuf.* **2019**, *4* (3), 245–267. https://doi.org/10.1007/s40964-019-00077-7.
(31) Lee, J. M.; Sing, S. L.; Zhou, M.; Yeong, W. Y. 3D Bioprinting Processes: A Perspective on Classification and Terminology. *Int. J. Bioprinting* **2018**, *4* (2). https://doi.org/10.18063/ijb.v4i2.151.
(32) Lewis, J. A. Direct Ink Writing of 3D Functional Materials. *Adv. Funct. Mater.* **2006**, *16* (17), 2193–2204. https://doi.org/10.1002/adfm.200600434.
(33) Lewis, J. A.; Gratson, G. M. Direct Writing in Three Dimensions. *Mater. Today* **2004**, *7* (7–8), 32–39. https://doi.org/10.1016/S1369-7021(04)00344-X.
(34) ISO/ASTM. *Standard Terminology for Additive Manufacturing — General Principles — Terminology, 52900:2015(E)*.
(35) Jing, X.; Zhao, W.; Lan, L. Effect of Particle Size on Electric Conducting Percolation Threshold in Polymer/Conducting Particle Composites. *J. Mater. Sci. Lett.* **2000**, *19* (5), 377–379. https://doi.org/10.1023/A:1006774318019.
(36) Hall, R. A. Computer Modelling of Rubber-Toughened Plastics: Random Placement of Monosized Core-Shell Particles in a Polymer Matrix and Interparticle Distance Calculations. *J. Mater. Sci.* **1991**, *26* (20), 5631–5636. https://doi.org/10.1007/PL00020435.
(37) Auras, R. A.; Lim, L. T.; Selke, S. E. M.; Tsuji, H. *Poly (Lactic Acid): Synthesis, Structures, Properties, Processing, and Applications*; John Wiley & Sons, 2011; Vol. 10.
(38) Roth, C. B. *Polymer Glasses*; CRC Press, 2016.
(39) Vyavahare, O.; Ng, D.; Hsu, S. L. Analysis of Structural Rearrangements of Poly(Lactic Acid) in the Presence of Water. *J. Phys. Chem. B* **2014**, *118* (15), 4185–4193. https://doi.org/10.1021/jp500219j.
(40) Naga, N.; Yoshida, Y.; Inui, M.; Noguchi, K.; Murase, S. Crystallization of Amorphous Poly(Lactic Acid) Induced by Organic Solvents. *J. Appl. Polym. Sci.* **2011**, *119* (4), 2058–2064. https://doi.org/10.1002/app.32890.
(41) Cai, H.; Dave, V.; Gross, R. A.; McCarthy, S. P. Effects of Physical Aging, Crystallinity, and Orientation on the Enzymatic Degradation of Poly(Lactic Acid). *J. Polym. Sci. Part B Polym. Phys.* **1996**, *34* (16), 2701–2708. https://doi.org/10.1002/(SICI)1099-0488(19961130)34:16<2701::AID-POLB2>3.0.CO;2-S.
(42) Cui, L.; Imre, B.; Tátraaljai, D.; Pukánszky, B. Physical Ageing of Poly(Lactic Acid): Factors and Consequences for Practice. *Polymer* **2020**, *186*, 122014. https://doi.org/10.1016/j.polymer.2019.122014.
(43) Kovacs, A. J. Transition vitreuse dans les polymères amorphes. Etude phénoménologique. *Fortschritte Hochpolym.-Forsch.* **1964**, *3* (3), 394–507. https://doi.org/10.1007/BF02189445.
(44) Kwon, M.; Lee, S. C.; Jeong, Y. G. Influences of Physical Aging on Enthalpy Relaxation Behavior, Gas Permeability, and Dynamic Mechanical Property of Polylactide Films with

Various D-Isomer Contents. *Macromol. Res.* **2010**, *18* (4), 346–351. https://doi.org/10.1007/s13233-010-0410-7.

(45) Bor, Y.; Alin, J.; Hakkarainen, M. Electrospray Ionization-Mass Spectrometry Analysis Reveals Migration of Cyclic Lactide Oligomers from Polylactide Packaging in Contact with Ethanolic Food Simulant: ESI-MS ANALYSIS OF MIGRATION FROM PLA PACKAGING. *Packag. Technol. Sci.* **2012**, *25* (7), 427–433. https://doi.org/10.1002/pts.990.

(46) Lu, H.; Madbouly, S. A.; Schrader, J. A.; Srinivasan, G.; McCabe, K. G.; Grewell, D.; Kessler, M. R.; Graves, W. R. Biodegradation Behavior of Poly(Lactic Acid) (PLA)/Distiller's Dried Grains with Solubles (DDGS) Composites. *ACS Sustain. Chem. Eng.* **2014**, *2* (12), 2699–2706. https://doi.org/10.1021/sc500440q.

(47) Dale, R.; Squirrell, D. J. A Rapid Method for Assessing the Resistance of Polyurethanes to Biodeterioration. *Int. Biodeterior.* **1990**, *26* (6), 355–367. https://doi.org/10.1016/0265-3036(90)90001-N.

(48) Sarasa, J.; Gracia, J. M.; Javierre, C. Study of the Biodisintegration of a Bioplastic Material Waste. *Bioresour. Technol.* **2009**, *100* (15), 3764–3768. https://doi.org/10.1016/j.biortech.2008.11.049.

(49) Eren, H. A.; Avinc, O.; Uysal, P.; Wilding, M. The Effects of Ozone Treatment on Polylactic Acid (PLA) Fibres. *Text. Res. J.* **2011**, *81* (11), 1091–1099. https://doi.org/10.1177/0040517510397576.

(50) Eller, H.; Denoth, A. A Capacitive Soil Moisture Sensor. *J. Hydrol.* **1996**, *185* (1–4), 137–146. https://doi.org/10.1016/0022-1694(95)03003-4.

(51) Dean, T. J.; Bell, J. P.; Baty, A. J. B. Soil Moisture Measurement by an Improved Capacitance Technique, Part I. Sensor Design and Performance. *J. Hydrol.* **1987**, *93* (1–2), 67–78. https://doi.org/10.1016/0022-1694(87)90194-6.

(52) Dean, R. N.; Rane, A. K.; Baginski, M. E.; Richard, J.; Hartzog, Z.; Elton, D. J. A Capacitive Fringing Field Sensor Design for Moisture Measurement Based on Printed Circuit Board Technology. *IEEE Trans. Instrum. Meas.* **2012**, *61* (4), 1105–1112. https://doi.org/10.1109/TIM.2011.2173041.

TOC graphic

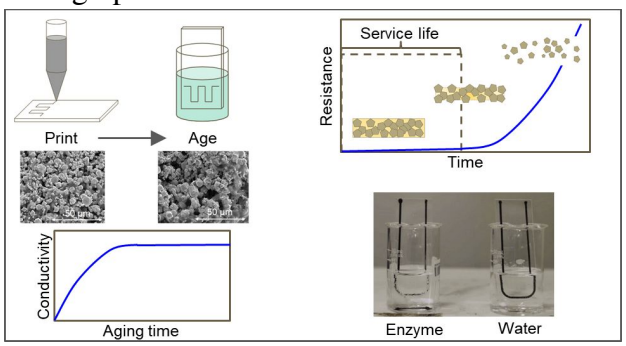
Print
Age
Service life
Resistance
Time
Conductivity
Aging time
Enzyme
Water